Axial Flux Permanent Magnet Vernier Machine with Single-wound Dual-stator and Spoke Permanent Magnet Rotor for Electric Vehicle In-wheel Traction

Ali Mohammadi¹, Yaser Chulaee¹, Aaron M. Cramer², Ion Boldea³, and Dan M. Ionel¹

¹SPARK Laboratory, ECE Department, University of Kentucky, Lexington, KY, USA

²ECE Department, University of Kentucky, Lexington, KY, USA

³Department of Electrical Engineering, The Polytechnic University of Timisoara, Timisoara, Romania alimohammadi@uky.edu, yaser.chulaee@uky.edu, aaron.cramer@uky.edu ion.boldea@upt.ro, dan.ionel@ieee.org

Abstract—In this paper, a dual-stator axial flux permanent magnet machine with a spoke-type rotor for electric vehicle applications is investigated. The rotor PMs are positioned in a spoke-type field-concentrating arrangement, which provides high flux concentration. Two stators—one stator configuration with double-layer wound coils and another without winding—are employed. The usage of single-layer wound coils is possible in this topology, and by using this type of winding it is possible to implement advanced in-slot cooling systems. Analytical and electromagnetic finite element analysis (FEA) studies considering its geometrical and electrical properties have been performed on this machine. The performance indices for the traction application based on the analytically calculated torque-speed characteristic, and FEA calculated torque versus torque angle have been assessed, and the results indicate that by using the proposed flux weakening methods, this machine can perform the flux weakening and operate in the constant power region of the torque-speed characteristic.

Index Terms—Axial flux vernier machine, spoke rotor, finite element analysis, flux weakening, d-axis inductance, electrical vehicles, in-wheel motor.

I. INTRODUCTION

In the automobile industry, great emphasis has been dedicated in recent decades to the development of electric vehicles (EVs) and hybrid electric vehicles (HEVs). Because of the ease of energy conversion and the minimization of mechanical losses, EVs powered by in-wheel motors have a suitable structure for this application. Multiple driving modes can benefit from in-wheel motors. When compared to standard electric vehicles with a single centrally located motor and automobiles powered by internal combustion engines, electric vehicles with four independently-driven in-wheel motors are advantageous in terms of transmission efficiency, and as a result, the interest in in-wheel motors has increased [1], [2].

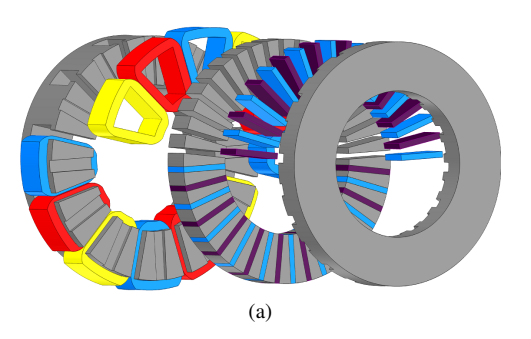
Permanent magnet synchronous machines (PMSM) with high specific torque have been a major subject of ongoing research, e.g. [3]–[5]. Among different topologies, machines of the spoke type in axial-flux (AF) configurations have been reported to be suitable in this respect and were considered appropriate candidates for direct-drive low-speed applications,

such as in-wheel traction and wind turbine generators [6], [7]. The advantages of spoke-type motors are high rotor polarities that provide opportunities for magnetic flux concentration, combined with a very low number of stator coils, which may simplify the manufacturing of stator windings [8], [9]. The design of a double-rotor, axial-flux switched reluctance motor for a light electric vehicle (LEV) propulsion application is discussed in [10], where the motor design is adjusted for performance and manufacturability, with a novel structural winding proposed to maximize the axial space available for conductors.

Typically, traditional permanent magnet synchronous machines (PMSMs) can achieve constant power operation by introducing a negative current in the d-axis. However, this method is often limited to a narrow range of speeds. Constant power operation methods have been explored in [11] for a coreless axial flux permanent magnet synchronous machine and two novel methods are proposed, namely current weakening and relative winding rotation. A study for suitable motor choices for the front and rear wheels of a dual-motor all-wheel drive EV for optimal torque distribution and high efficiency has been presented in [12].

The effectiveness of different cooling designs for axial-flux permanent magnet (AFPM) machines, which are preferred for high power and torque densities in applications with space limitations has been shown in [13]. The significance of cooling in high power density AFPMs is highlighted in [14], in which ventilated-type axial-flux permanent magnet machines use air cooling to maintain the temperature of the rotor magnets below critical limits.

In this paper, an axial flux permanent magnet vernier machine for electric vehicle in-wheel traction has been investigated. The motor topology and construction are discussed in section II. In section III the in-wheel model for traction application is introduced. The constant power operation of the machine is shown in section IV, and section V provides further discussions about flux weakening. Finally, the main findings and conclusions of this paper are summarized in section VI.



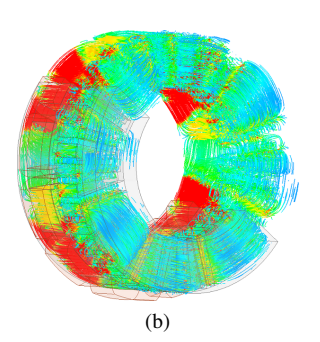




Fig. 1. The electric motor topology for in-wheel traction (a) exploded view of the MAGNUS machine with double stators and the rotor in the middle,(b) the flux density distribution of the machine at the rated loading (c) the in-wheel schematic for the electric motor and the vehicle wheel.

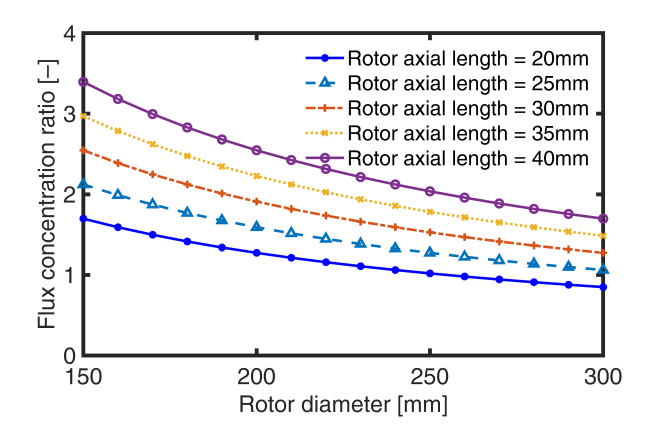


Fig. 2. Flux concentration ratio of the studied model versus rotor diameter for different values of rotor axial length. The highest to lowest flux concentration ratios are at lower to higher radii, respectively.

II. MOTOR TOPOLOGY, CONSTRUCTION, AND REFERENCE PROTOTYPE

The electric machine in this paper, as shown in Fig. 1(a) has two stators. The main stator and the auxiliary stator, where both have 12 teeth and split poles. The main stator has 3 phases and 12 coils wound on the teeth in a double-layer arrangement and the auxiliary stator is profiled similarly to the main stator, without any coils in its slots. It is important to note that in this machine different slot and pole combinations are possible.

There is a wide range of options for slot-pole combinations that can be used for this machine. To determine the number of rotor poles required for a three-phase machine, two conditions need to be considered. The first condition states that there must be an odd number of PM poles facing each stator tooth to ensure that only PM poles of one polarity contribute to the phase flux linkage at any given time. The second condition requires a phase shift of 120 degrees between the phases. These conditions can be expressed as:

$$P_r > nT_s, \tag{1}$$

where, the value of n is given depending on the number of auxiliary stator teeth t_s , while P_r represents the number of rotor poles, and T_s is the number of main stator teeth that can

be used for a range of slot-pole combinations in this machine as:

$$n = 2t_s - 1, (2)$$

The second condition, which needs to be considered is expressed as:

$$P_r = \frac{2}{3}T_s k_1,\tag{3}$$

where, the value of k_1 can be any number except for multiples of 3. The motor under study in this paper has 12 main stator teeth and 2 auxiliary teeth, and the first value of P_r that meets the requirements is 40 poles.

The structure of this machine allows the use of a single-layer coil per slot configuration. For the in-wheel traction, as shown in Fig. 1(c), the machine structure benefits from the ability to have direct cooling for the main stator winding. The special structure of the stator allows for advanced cooling system implementations such as micro-channels in the middle of the slot, which allows for high values of the current density in the stator winding.

The rotor of this electrical machine has 40 permanent magnets (20 pole pairs), which are inserted in the rotor in a spoke-type configuration resulting in a very high flux concentration. The effect of this high flux concentration can be shown by studying the machine at different conditions. One of the studies specifically performed in this paper was to show the flux concentration ratio at different positions in the radial direction in the machine airgap. The results of this study are depicted in Fig. 2. The flux concentration ζ for a double-stator axial flux spoke topology can be defined as:

$$\zeta = \frac{h_{PM}}{\tau_p},\tag{4}$$

where, h_{PM} is the length of the PM, τ_p the rotor pole pitch, i.e., rotor outer circumference πD_s divided by the number of permanent magnets n_{PM} .

The effect of rotor axial length on the flux concentration ratio is also shown in Fig. 2. The increase in the rotor axial length directly increases the flux concentration ratio, while the value of this ratio decreases as the circumference of the calculations increases. In this model, the inner and outer diameters of the rotor are 150 and 300 mm, respectively.



Fig. 3. The electric motor prototype for in-wheel traction (a) The assembled prototype, and (b) from left to right are the auxiliary stator with profiled teeth, rotor with spoke permanent magnets, and active stator wound with double-layer coils and profiled teeth. The profiled teeth in the stators improve the torque production of the machine.

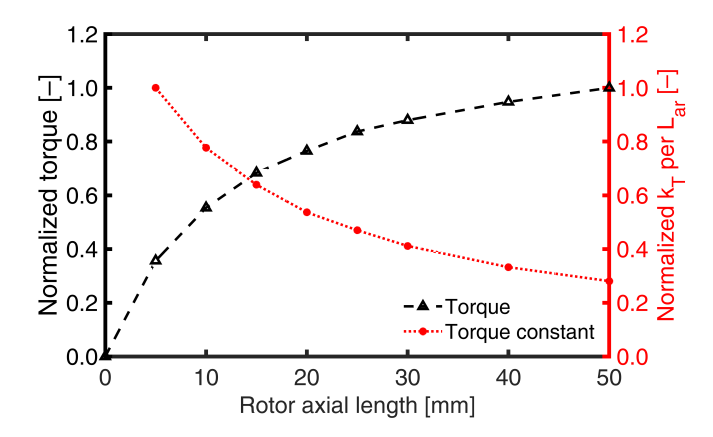


Fig. 4. Normalized electromagnetic torque and normalized torque constant per rotor unit axial length versus the rotor axial length at the rated current loading; shows the rotor axial length where saturation affects the torque characteristics.

The paper utilizes a machine as the basis for its design, and this machine has been successfully prototyped, as demonstrated in Fig. 3. The prototype was developed and introduced in a previously published paper as MAGNUS [15]. The fully assembled prototype is depicted in Fig. 3(a), providing a clear visual representation of the machine. Moreover, the three primary components of the prototype are shown separately in Fig. 3(b), providing an in-depth look into its components. This prototype is essential to this paper, as it serves as a calibrated model for the design. With this calibrated model, the performance of the machine, its capabilities, and its limitations can be studied.

III. DESIGN FOR IN-WHEEL APPLICATION

Depending on the weight of the electric vehicle, multiple specifications for the in-wheel traction motors have been developed. Electric motors with 400 Nm of peak torque and a range of 20 to 40 kW of peak power can be used in lightweight vehicles that can be fully electric vehicles or even hybrid. In-wheel motors developed with 700 Nm of peak torque and 75 kW of peak power are used in heavier vehicles, including passenger cars. For trains and buses, more powerful in-wheel motors have been designed with more than 1,000 Nm of peak torque and 90 kW of peak power. In this paper, the model of

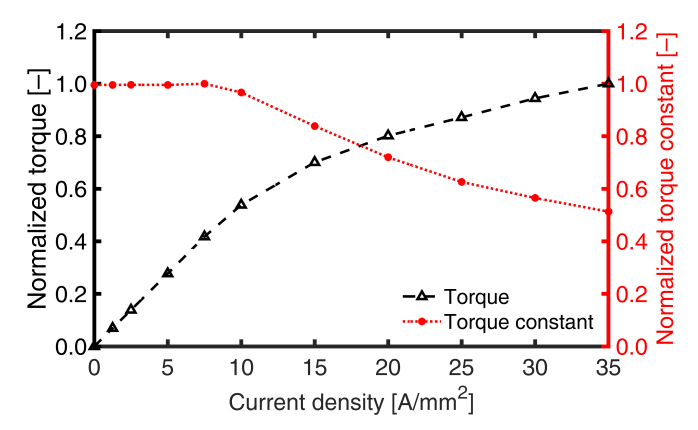


Fig. 5. The normalized electromagnetic torque and torque constant curves versus different current density values for the model with 300 mm diameter, where the current densities higher than 10 A/mm² cause saturation in the machine.

the prototype is studied for different variations of geometrical and electrical characteristics. In this model, an overall outer diameter of 300 mm has been considered. The normalized characteristic of electromagnetic torque versus current density is as shown in Fig. 5. These results were obtained using the 3D finite element analysis, using ANSYS Electronics software [16]. In this figure, the second axis shows the normalized torque constant, and it is defined as the ratio of the normalized electromagnetic torque to current density.

The normalized torque and torque constant curves of this model in Fig. 5 show the effect of saturation on the magnetic core for current densities higher than 10 A/mm². The torque and torque constant curves shown in this figure are normalized based on the 540 Nm peak torque produced by this model and a 50% overload at this point with respect to the continuous (rated) torque is considered. At the overload condition, the machine can deliver 85 kW as its peak electromagnetic power. This shows that the model in this paper can cover a wide range of applications for in-wheel traction.

When the rated current density is applied to the designed model with a rotor axial length (L_{ar}) of 30 mm, the normalized torque curve in Fig. 5 indicates that the effect of saturation becomes apparent as the axial length of the rotor

is increased. Specifically, at an axial length of 10 mm, the normalized torque constant experiences a reduction due to the saturation effect.

IV. CONSTANT POWER OPERATION

In traction applications, a critical aspect of the machine's performance is the torque versus speed curve [17]. Ideally, this curve should indicate a constant torque up to the base speed, which is the maximum speed where the machine's voltage is equal to the inverter's maximum voltage. At this point, the voltage limitation of the inverter is reached, and further increases in speed would require constant power operation. The d-axis inductance of an ideal non-salient machine with infinite speed is 0.707 p.u. To maintain this constant power operation, the terminal voltage necessary for running the machine at a specific angular speed ω can be computed as:

$$V = \omega \sqrt{(\lambda_{pm} + L_d I \cos(\beta))^2 + (\xi L_d I \sin(\beta))^2}, \quad (5)$$

where, λ_{pm} is the open-circuit flux linkage; L_d , the direct (d) axis inductance; L_q , the quadrature (q) axis inductance; I, the motor current; β , the torque angle, and $\xi = L_q/L_d$, the saliency ratio. The machine's electromagnetic torque can be expressed as:

$$T = \frac{m}{2} p[\lambda_{pm} I \sin(\beta) - \frac{1}{2} (\xi - 1) L_d I^2 \sin(2\beta)], \quad (6)$$

where, m is the number of phases and p number of poles.

The saliency ratio of the MAGNUS model is equal to one, therefore the reluctance torque is zero. In a PMSM, where there is no saliency, to decouple the d- and q-axis components of the current, the rotor reference frame-oriented control is employed. When $\xi=1$ the maximum torque per ampere (MTPA) is obtained when the d-axis current is driven to zero or β is maintained at 90 degrees with respect to the q-axis, as shown in Fig. 6. At higher speeds, a negative value of I_d can be used to reduce the terminal voltage, otherwise directly proportional to speed. The value of I_d is increased such that the total rms phase current is constant, i.e.:

$$I_d^2 + I_a^2 = I_s^2, (7$$

where, I_s is the phase current at 1 p.u. and this serves to reduce the torque, as it is directly proportional to I_q . The flux linkage reduces with increasing value of negative I_d (i.e. $90^o < \beta < 180^o$) such that the terminal voltage is constant. Furthermore, the torque profile of the model in this paper is depicted in Fig. 6; in this model, the saliency ratio is close to one, hence, d and q-axis inductances are almost equal, which can be seen in the electromagnetic torque curve where the maximum electromagnetic torque is at $\beta = 90^o$.

The analytically calculated torque-speed characteristics for different values of per-unit L_d and the dependence of the width of the constant power region on the d-axis inductance values are shown in Fig. 7. Lower values of per-unit inductance, lead to a narrower constant power region. The torque-speed characteristics were calculated assuming an available terminal voltage of 1 p.u. in machines with different values of per-unit inductances.

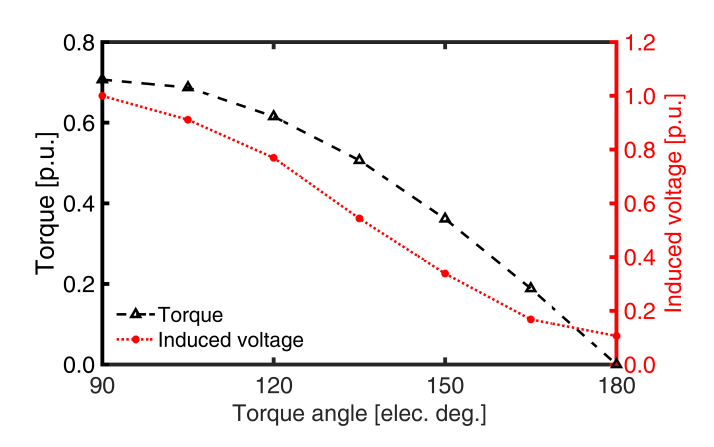


Fig. 6. The electromagnetic torque and per unit fundamental rms of the induced voltage characteristics of the model at the rated current loading and speed versus the torque angle. The graph indicates that due to non-saliency, the maximum electromagnetic torque occurs at 90 degrees with respect to the q-axis.

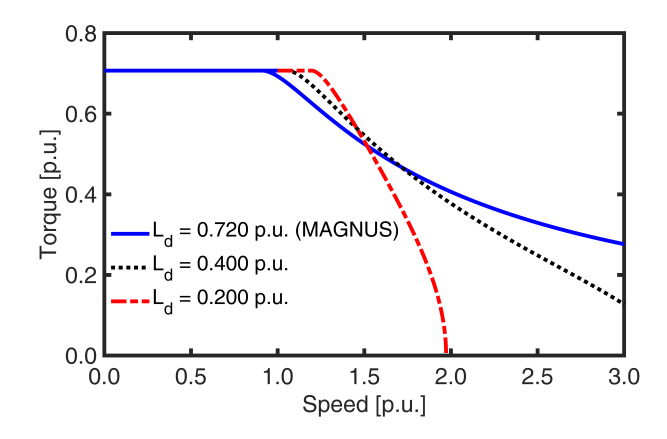


Fig. 7. Torque versus speed characteristics of MAGNUS model and examples of PMSMs with different values of the per-unit d-axis inductance. MAGNUS has a wide constant power operation region, which enables it to successfully maintain constant power.

V. DISCUSSION AND FUTURE WORKS

Flux weakening is an essential feature for traction machines, as it allows the machine to operate above the base speed while still maintaining the maximum terminal voltage. The machine under study in this paper has a high per-unit inductance and a wide constant operation region also shown in Fig. 7, while maintaining a constant voltage of 1 p.u. at higher speeds, and is able to perform flux weakening without the need to use other methods, which will be explained in the following.

One approach for flux weakening is using the current phase advance along with the mechanical rotation in the auxiliary stator. Mechanical flux weakening has been previously introduced for maintaining constant power for PMSMs in [18]. The auxiliary stator of MAGNUS can be mechanically rotated around its axis and by doing so; as shown in Fig. 8 the voltage can be reduced to 60% of its nominal value.

Other methods such as dynamic winding re-configuration can also be used to further reduce the machine's voltage for higher speeds. In one implementation, for example, the windings can be connected in series for operation in the

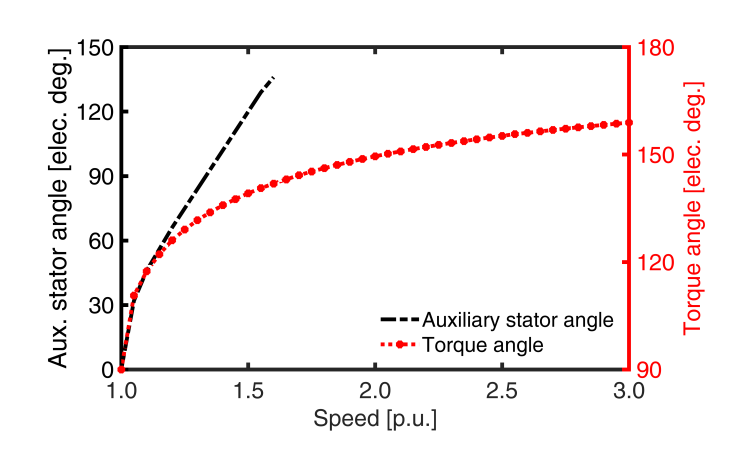


Fig. 8. Flux weakening mechanism by torque angle phase advance and the mechanical rotation of the auxiliary stator with respect to the main stator and the initial position of the rotor, which can result in 40% voltage reduction.

constant torque region of the torque-speed characteristics, and in parallel for operation in the constant power region.

The presented vernier machine has been designed specifically for in-wheel traction application. To enhance its performance, further improvements can be made by implementing a design optimization using the differential evolution algorithm along with 3D FEA. This optimization can be based on a specific driving cycle for traction application for required operation centroids of that driving cycle.

VI. CONCLUSION

The dual-stator spoke-type vernier machine that was studied is advantageous as permanent magnets used in the rotor have the spoke-type arrangement, which results in a high flux concentration ratio. The topology studied is able to perform with double-layer and single-layer coil configurations, where the latter enables the implementation of advanced cooling systems that are necessary for electric vehicle traction applications. The design considerations for a model and the prototype has been introduced and based on a specified design for the machine profile to meet the traction application requirements have been shown. Based on an analytical torque-speed characteristic for the per-unit values of direct axis inductance, the model that was introduced in this paper benefits from a high per-unit daxis inductance, which enables a wide constant power operation. More flux weakening methods, i.e. using the mechanical rotation of the auxiliary stator with respect to the main stator along with the current phase advance has been introduced.

ACKNOWLEDGMENT

This paper is based upon work supported by the National Science Foundation (NSF) under Award No. #1809876. Any opinions, findings, conclusions, or recommendations expressed in this material are those of the authors and do not necessarily reflect the views of the NSF. The support of Ansys Inc., and University of Kentucky, the L. Stanley Pigman Chair in Power endowment is also gratefully acknowledged.

REFERENCES

- [1] A. Allca-Pekarovic, P. J. Kollmeyer, A. Forsyth, and A. Emadi, "Experimental characterization and modeling of a yasa p400 axial flux pm traction machine for electric vehicles," in 2022 IEEE Transportation Electrification Conference & Expo (ITEC), 2022, pp. 433–438.
- [2] X. Sun, Z. Shi, Y. Cai, G. Lei, Y. Guo, and J. Zhu, "Driving-cycle-oriented design optimization of a permanent magnet hub motor drive system for a four-wheel-drive electric vehicle," *IEEE Transactions on Transportation Electrification*, vol. 6, no. 3, pp. 1115–1125, 2020.
- [3] A. Fatemi, D. M. Ionel, M. Popescu, Y. C. Chong, and N. A. O. Demerdash, "Design optimization of a high torque density spoke-type pm motor for a formula e race drive cycle," *IEEE Transactions on Industry Applications*, vol. 54, no. 5, pp. 4343–4354, 2018.
- [4] Y. Chulaee, D. Lewis, A. Mohammadi, G. Heins, D. Patterson, and D. M. Ionel, "Circulating and eddy current losses in coreless axial flux pm machine stators with pcb windings," *IEEE Transactions on Industry Applications*, pp. 1–11, 2023.
- [5] A. Mohammadi and S. M. Mirimani, "Design of a novel pm-assisted synchronous reluctance motor topology using v-shape permanent magnets for improvement of torque characteristic," *IEEE Transactions on Energy Conversion*, vol. 37, no. 1, pp. 424–432, 2021.
- [6] F. Zhao, T. A. Lipo, and B.-I. Kwon, "A novel dual-stator axial-flux spoke-type permanent magnet vernier machine for direct-drive applications," *IEEE Transactions on Magnetics*, vol. 50, no. 11, pp. 1–4, 2014.
- [7] A. Mohammadi, O. A. Badewa, Y. Chulaee, D. M. Ionel, S. Essakiappan, and M. Manjrekar, "Direct-drive wind generator concept with non-rare-earth pm flux intensifying stator and reluctance outer rotor," in 2022 11th International Conference on Renewable Energy Research and Application (ICRERA). IEEE, 2022, pp. 582–587.
- [8] G. Heins, D. Ionel, and M. Thiele, "Winding factors and magnetic fields in permanent magnet brushless machines with concentrated windings and modular stator cores," in 2013 IEEE Energy Conversion Congress and Exposition, 2013, pp. 5048–5055.
- [9] R. Zhang, J. Li, R. Qu, and D. Li, "Analysis and design of triplerotor axial-flux spoke-array vernier permanent magnet machines," *IEEE Transactions on Industry Applications*, vol. 54, no. 1, pp. 244–253, 2018.
- [10] J. Gillies, T. Lambert, A. Emadi, and B. Bilgin, "Axial-flux switched reluctance motor design for a light electric vehicle application," in 2022 IEEE Transportation Electrification Conference and Expo (ITEC), 2022, pp. 790–795.
- [11] D. Lawhorn, N. Taran, V. Rallabandi, and D. M. Ionel, "A comparative study of constant power operation techniques for low inductance machines," in 2018 IEEE Transportation Electrification Conference and Expo (ITEC), 2018, pp. 638–643.
- [12] M. Oh and I. Husain, "Optimal torque distribution of dual-motor all-wheel drive electric vehicles for maximizing motor energy efficiency," in 2021 IEEE Transportation Electrification Conference and Expo (ITEC), 2021, pp. 188–193.
- [13] S. Jones-Jackson, R. Rodriguez, E. Sayed, C. Goldstein, C. Mak, A. Callegaro, M. Goykhman, and A. Emadi, "Design and analysis of stator cooling channels for an axial-flux permanent magnet machine," in 2021 IEEE Transportation Electrification Conference and Expo (ITEC), 2021, pp. 272–277.
- [14] I. Zaher, R. Rodriguez, E. Sayed, A. Callegaro, M. Goykhman, and A. Emadi, "Effect of rotor geometry on rotor air cooling of a ventilated axial-flux permanent magnet machine," in 2021 IEEE Transportation Electrification Conference and Expo (ITEC), 2021, pp. 77–82.
- [15] M. G. Kesgin, P. Han, D. Lawhorn, and D. M. Ionel, "Analysis of torque production in axial-flux vernier pm machines of the magnus type," in 2021 IEEE International Electric Machines & Drives Conference (IEMDC), 2021, pp. 1–5.
- [16] M. Rosu, P. Zhou, D. Lin, D. M. Ionel, M. Popescu, F. Blaabjerg, V. Rallabandi, and D. Staton, "Multiphysics Simulation by Design for Electrical Machines, Power Electronics and Drives", J. Wiley - IEEE Press, 2017.
- [17] D. Ionel, J. Eastham, and T. Betzer, "Finite element analysis of a novel brushless dc motor with flux barriers," *IEEE Transactions on Magnetics*, vol. 31, no. 6, pp. 3749–3751, 1995.
- [18] I. Boldea and L. N. Tutelea, "Pmsm with rotor pm mechanical flux-weakening (mfw) to zero for an 150kw, 600vdc, 500–6000 rpm drive: Preliminary design with key validation," in 2016 XXII International Conference on Electrical Machines (ICEM), 2016, pp. 1995–2001.